Experimental Cell Research **281,** 50–62 (2002)
doi:10.1006/excr.2002.5651

Human Heparanase Is Localized within Lysosomes in a Stable Form

Orit Goldshmidt,*[,3] Liat Nadav,§[,3] Helena Aingorn,* Cohen Irit,* Naomi Feinstein,‖ Neta Ilan,¶[,]‡ Eli Zamir,** Benjamin Geiger,** Israel Vlodavsky,*[,]‡[,1] and Ben-Zion Katz§[,2]

*Department of Oncology, Hadassah-Hebrew University Hospital, Jerusalem; §Department of Hematology, Tel-Aviv Sourasky Medical Center, Tel-Aviv; ‖Electron Microscopy Unit, Institute of Life Sciences, Hebrew University of Jerusalem; ¶InSight Ltd., Rehovot; **Department of Cellular and Molecular Biology, Weizmann Institute of Science, Rehovot; and ‡Vascular Biology Research Center, the Bruce Rappaport Faculty of Medicine, Technion, Haifa, 31096, Israel

Heparanase is an endo-β-D-glucuronidase involved in degradation of heparan sulfate (HS) and extracellular matrix (ECM) of a wide range of cells of vertebrate and invertebrate tissues. The enzymatic activity of heparanase is characterized by specific intrachain cleavage of glycosidic bonds with a hydrolase mechanism. This enzyme facilitates cell invasion and hence plays a role in tumor metastasis, angiogenesis, inflammation, and autoimmunity. Although the expression pattern and molecular properties of heparanase have been characterized, its subcellular localization has not been unequivocally determined. We have previously suggested that heparanase subcellular localization is a major determinant in regulating the enzyme's biological functions. In the present study we examined heparanase localization in three different cell types, utilizing immunofluorescent staining and electron microscopy. Our results indicate that heparanase is localized primarily within lysosomes and the Golgi apparatus. A construct composed of heparanase cDNA fused to green fluorescent protein, utilized in order to visualize the enzyme within living cells, confirmed its localization in acidic vesicles. We suggest that following synthesis, heparanase is transported into the Golgi apparatus and subsequently accumulates in a stable form within the lysosomes, where it functions in HS turnover. The lysosomal compartment may also serve as a site for heparanase confinement within the cells, limiting its secretion and uncontrolled extracellular activities associated with tumor metastasis and angiogenesis.

Key Words: **heparan sulfate proteoglycans; heparanase; heparanase-GFP; lysosomes; signal peptide; MCF7 breast carcinoma.**

INTRODUCTION

Heparan sulfate proteoglycans (HSPGs) on cell surfaces and in basement membranes and extracellular matrices (ECM) affect biological processes by interacting with various ECM components and a large number of biologically active molecules [1, 2]. HSPGs can thus influence a variety of normal and pathological processes, involving cell adhesion, migration, and invasion [1–4]. The importance and multifunctional roles of HSPGs in the physiology of cells and tissues make their cleavage an essential factor in the regulation of the integrity and functional state of organs. Enzymatic degradation of heparan sulfate (HS) is therefore likely to be involved in fundamental biological processes ranging from pregnancy, morphogenesis, and normal development to inflammation, angiogenesis, and cancer metastasis [5–10]. Despite earlier reports on the existence of several distinct mammalian HS degrading endoglycosidases (heparanases), the cloning of the same gene by several groups suggests that mammalian cells express predominantly a single functional heparanase enzyme [6, 11–13]. The HS chains are cleaved by heparanase at only a few sites, yielding HS fragments of still appreciable size (10–20 sugar units) [14]. The heparanase mRNA and protein are preferentially expressed in metastatic cell lines and human tumor tissues [6, 8–12, 15]. Moreover, enhanced heparanase mRNA expression correlates with reduced postoperative survival of cancer patients [16, 17]. Overexpression of the heparanase cDNA in low-metastatic tumor cells conferred a high metastatic potential in experimental animals, resulting in an increased rate of mortality [6]. The heparanase enzyme also releases ECM-resident angiogenic factors *in vitro* and its overexpression induces an angiogenic response *in vivo* [18]. While several studies have reported heparanase cloning, molecular properties, expression, and involvement in cancer progression, heparanase regulation and subcellular localization were not thoroughly investigated. Heparanase activity was first isolated from rat liver lysosomes [19] and has been demonstrated in both

[1] To whom correspondence and reprint requests should be addressed at Department of Oncology, Hadassah Hospital, POB 12000, Jerusalem 91120, Israel. Fax: 972-2-6422794. E-mail: vlodavsk@cc.huji.ac.il.

[2] Dedicated to the memory of Professor Amiram Eldor (who died November 2001 in a tragic airplane crash), whose inspiration, wisdom, and encouragement contributed to the accomplishment of this study.

[3] These authors contributed equally to this study.

0014-4827/02 $35.00

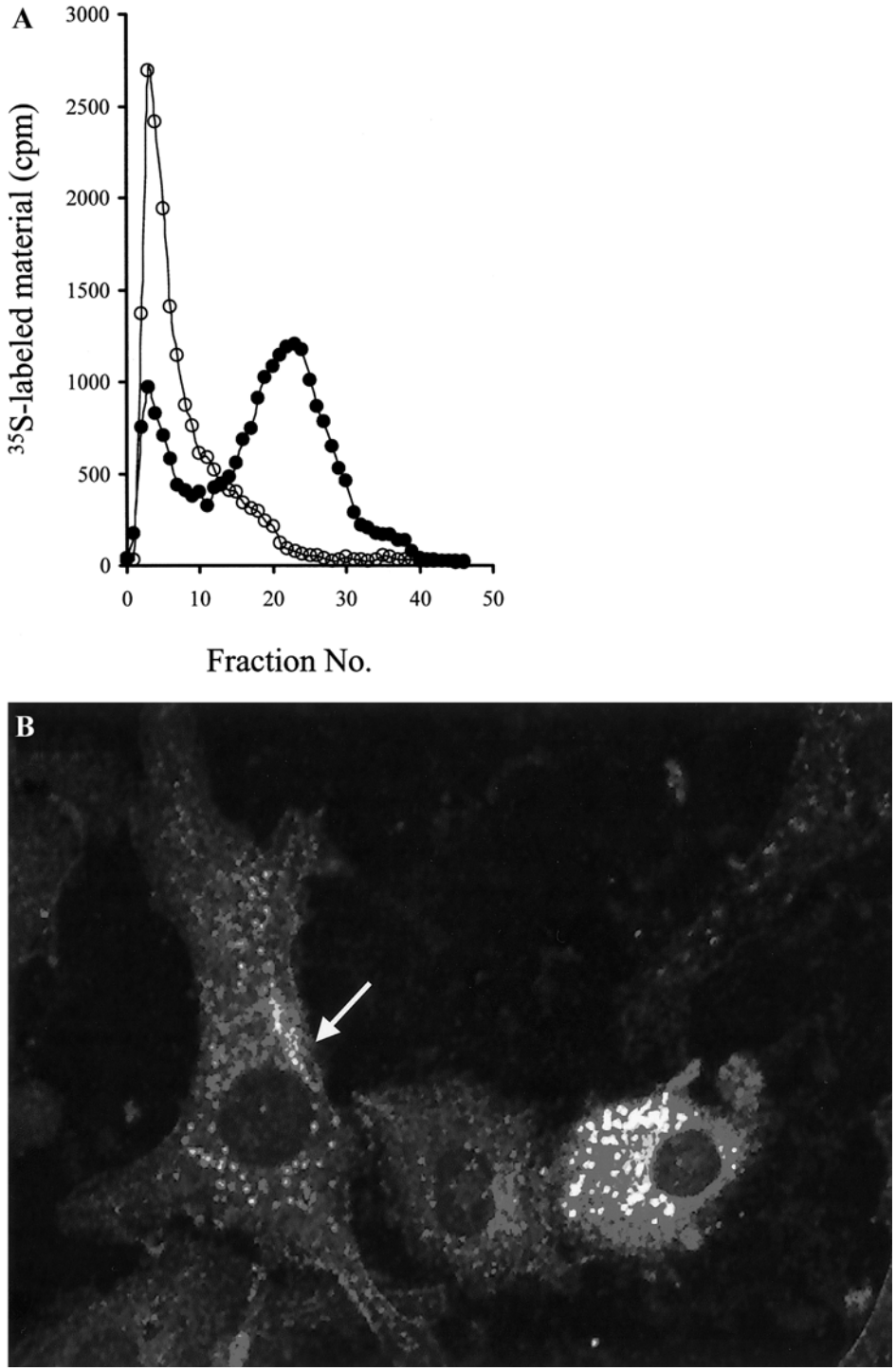

FIG. 1. Heparanase activity and cellular localization in transfected C6 glioma cells. (A) Cell lysates of C6 glioma cells transfected with human heparanase (H-*hpa*) (●) or mock transfected (○) were incubated (24 h, pH 6.0, 2×10^6 cells) on sulfate-labeled ECM. Labeled degradation fragments released into the incubation medium were analyzed by gel filtration on Sepharose 6B, as described under Materials and Methods. (B) Pooled populations of C6 glioma cells transfected with H-*hpa* cDNA were subjected to indirect immunofluorescence staining with monoclonal antiheparanase antibodies (mAb 130) followed by Cy3-conjugated goat antimouse antibody, as described under Materials and Methods. Cells transfected with H-*hpa* cDNA displayed primarily a perinuclear granular staining (arrow). Mock-transfected C6 glioma cells were used as control and showed no staining (not shown).

lysosomal and endosomal cellular compartments [20–23]. Previous studies identified heparanase activity in tertiary granules within neutrophiles, where it colocalized with gelatinase [24, 25]. In these early experiments the heparanase cellular localization was characterized by cell fractionation and by using antibodies that identified a 96-kDa protein [24]. Cloning and expression of the mammalian heparanase, however, revealed molecular weights of 65 kDa for the proenzyme and 50 kDa for the processed, highly active heparanase [26], questioning the specificity of these antibodies. The availability of recombinant heparanase enabled the development of monoclonal and polyclonal anti-heparanase antibodies, which were utilized to identify heparanase expression in cell lines and human tissues [6, 15–17], and the investigation of its localization in transfected cells [27]. The objective of the present study was to determine the subcellular localization of heparanase and better elucidate its routing within the cells. Using confocal and electron microscopies, as well as heparanase-GFP fusion protein, we have identified heparanase predominantly within lysosomes of both normal and malignant cells. We have also identified heparanase within the Golgi apparatus and demonstrated that the integrity of the Golgi is essential for the generation of an active enzyme.

MATERIALS AND METHODS

Antibodies. Monoclonal mouse antihuman heparanase antibodies (mAb 130) directed against the C-terminus of the 50-kDa active enzyme were obtained (Insight Ltd., Rohovot, Israel) as previously described [6]. Cy2-, Cy3-, or Alexa-conjugated goat antimouse antibodies were from Jackson Laboratories (Bar Harbor, ME).

Generation of heparanase-GFP fusion protein. Heparanase-GFP fusion protein was designed using standard molecular biology methods [28] and generated through the insertion of a unique *Eco*RV restriction site at the 3′ end of heparanase cDNA (upstream the termination codon) into the already described heparanase expression vector pHep2 [6]. Heparanase C-terminus was amplified by PCR, using pHep2 as a template. The sense primer, 5′-AGCCGAGGTTACCCTATCCTTTTTC-3′, contained the *Bst*EII restriction site, followed by a complementary sequence encoding for heparanase downstream to the restriction site. The antisense primer, 5′-ACCGCCCTCGAGTTCTGGTCAGATATCGATGCAAGCAGCAACTTT-3′, contained the *Xho*I restriction site, termination codon, and *Eco*RV restriction site, followed by a complementary sequence coding for heparanase upstream to the termination codon. The PCR product and the pHep2 plasmid were both restricted with *Xho*I and *Bst*EII, extracted from a preparative gel, and ligated. The recombinant plasmid was identified by the restriction enzymes *Eco*RV, *Xho*I, and *Bst*EII (restricting the insert) and gel electrophoresis. GFP cDNA was amplified with the addition of two restriction sites, *Eco*RV and *Xho*I, using a previously described GFP expression vector as a template [29]. The sense primer, 5′-CGCATCGATATCATGGTGAGCAAGGGCGAG-3′, contained the *Eco*RV restriction site, followed by a complementary sequence coding for GFP downstream to its initiation codon. The antisense primer, 5′-TGTGCCCTCGAGTTACTTGTACAGTGCGTC-3′, contained the *Xho*I restriction site followed by a complementary sequence coding for GFP upstream to its termination codon. The PCR product and the plasmid coding for heparanase were both restricted with *Xho*I and *Eco*RV and then extracted from a preparative gel. After ligation, the recombinant plasmid was identified by restriction analysis with *Xho*I, *Bst*EII, and *Eco*RV. The sequence of the pHep-GFP construct was confirmed by automated nucleotide sequencing. The resulting pHep-GFP is driven by the CMV promoter and it expresses in frame the complete heparanase cDNA followed by the GFP coding sequence. The previously described plasmids pHep2 and pGFP were utilized as controls [6, 29].

Cells and transfection procedures. Human foreskin fibroblasts were kindly provided by Dr. Susan S. Yamada (NIDCR, NIH, Bethesda, MD). Cells were maintained in Dulbecco's modified Eagle's medium (DMEM, 1 g of glucose/liter) supplemented with 1 mM glutamine, 50 μg/ml of streptomycin, 50 U/ml of penicillin, and 10% heat-inactivated bovine serum (Biological Industries, Beit-Haemek, Israel) at 37°C in a 5% humidified incubator. Electroporation of the cells was performed at 170 V and 950 μF utilizing a Bio–Rad Gene-Pulser (Hercules, CA), with a thymidine block, as previously described [30]. Transient transfection was performed using 30 μg of DNA for each plasmid, and protein expression was examined 48 h later. C6 rat glioma cells were cultured in DMEM (4.5 g of glucose/liter) supplemented with glutamine, antibiotics, and 10% fetal calf serum (FCS). MCF7 and MDA-231 human breast carcinoma cells were cultured in RPMI medium supplemented with 10% FCS, glutamine, and antibiotics. For transfection, H-*hpa* cDNA was subcloned into pcDNA3 plasmid (Invitrogen, NV Leek, Netherlands) at the *Eco*RI site as described [6, 27]. C6 rat glioma cells (5×10^6 cells/10-cm dish) were incubated (48–72 h, 37°C) with a total of 1–2 μg of DNA and 6 μl of FuGene transfection reagent (Boehringer, Mannheim, Germany) in 94 μl of Optimem (GibcoBRL, Rockville, MD). Transfected cells were selected with 800 μg/ml of G418 and stable populations of heparanase expressing cells were obtained [27]. Cultures of bovine corneal endothelial cells were established from steer eyes and maintained in DMEM (1 g of glucose/liter) supplemented with 5% newborn calf serum and 10% FCS, as described [31].

Preparation of dishes coated with ECM. Bovine corneal endothelial cells were plated into 35-mm tissue culture dishes and cultured as described above, except that 4% dextran T-40 was included in the growth medium [31, 32]. $Na_2{}^{35}SO_4$ (25 μCi/ml) (Amersham, Buckinghamshire, UK) was added on days 2 and 5 after seeding and the cultures were incubated with the label without medium change. On day 12, the subendothelial ECM was exposed by dissolving the cell layer with PBS containing 0.5% Triton X-100 and 20 mM NH_4OH, followed by four washes with PBS [31, 32]. The ECM remained intact, free of cellular debris, and firmly attached to the entire area of the tissue culture dish.

Heparanase activity. Cells (2×10^6 cells/ml) were lysed by three cycles of freezing and thawing in heparanase reaction solution (0.15 M NaCl, 20 mM phosphate-citrate buffer, pH 5.8, 1 mM dithiothreitol (DTT), 1 mM $CaCl_2$). Cell lysates were incubated (24 h, 37°C, pH 5.8) with ^{35}S-labeled ECM, the incubation medium was centrifuged, and the supernatant containing sulfate-labeled degradation fragments was analyzed by gel filtration on a Sepharose CL-6B column (0.9×30 cm). Fractions (0.2 ml) were eluted with PBS and their radioactivity was counted in a β-scintillation counter [6, 32]. Degradation fragments of HS side chains were eluted from Sepharose 6B at $0.5 < K_{av} < 0.8$ (fractions 15–35, peak II). Nearly intact HSPGs were eluted just after the V_0 ($K_{av} < 0.2$, fractions 1–10, peak I) [6, 32]. Each experiment was performed at least three times and the variation in elution positions (K_{av} values) did not exceed $\pm$ 15%.

Indirect immunofluorescence. Cultured primary human foreskin fibroblasts and C6 rat glioma and MDA-231 cells were stained by indirect immunofluorescence as previously described [27, 33]. Cells were fixed with either acetone (−20°C, 5 min) or 4% formaldehyde in PBS for 20 min and, when stated, permeabilized with 0.5% Triton X-100 in PBS for 5 min. The cells were then incubated with the indicated antibodies in PBS. Antiheparanase monoclonal antibodies

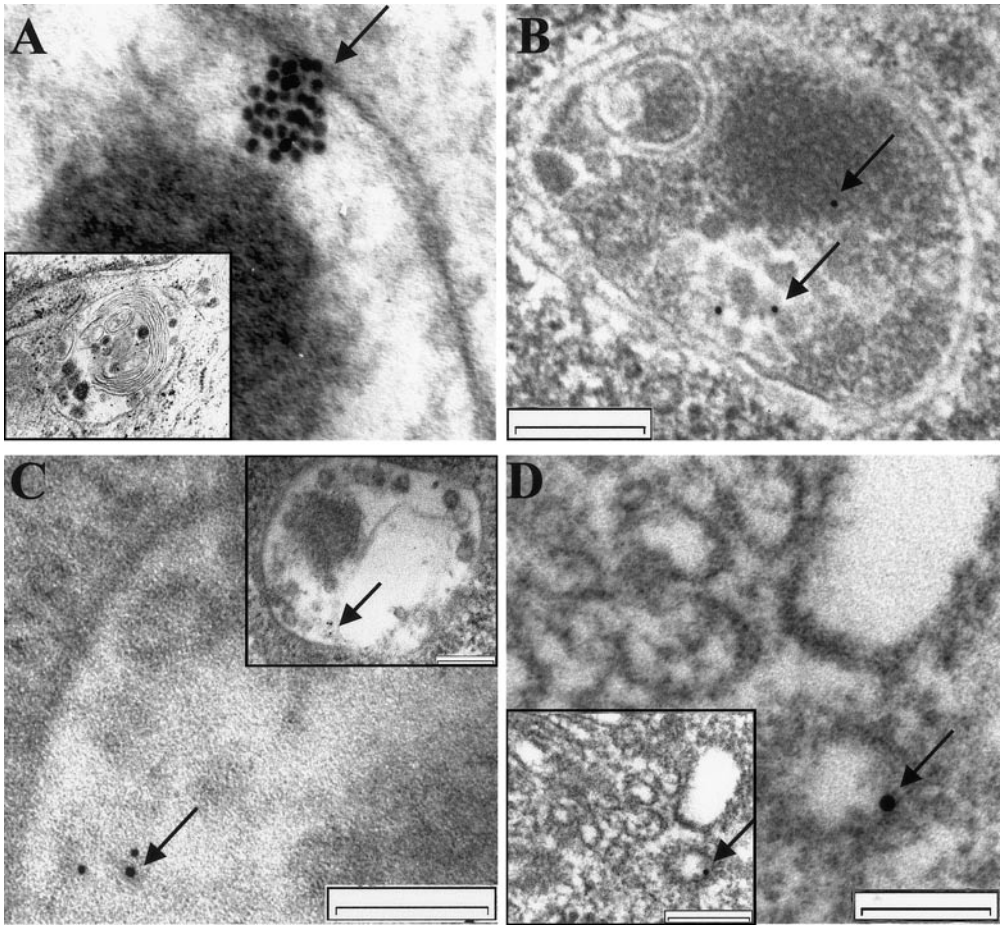

FIG. 2. Transmission electron micrographs of C6 glioma and MDA-231 breast carcinoma cells. (A) Rat C6 glioma cells transfected with H-*hpa*. (B–D) MDA-231 human breast carcinoma cells expressing endogenous heparanase. Cultured cells were processed for electron microscopy and heparanase was visualized using antihuman heparanase mAb 130 followed by antimouse IgG-conjugated gold particles, as described under Materials and Methods. Heparanase (arrows) is localized within lysosomes (A–C) and in the Golgi apparatus (D). Bars, 200 nm (B), 100 nm (C and D), and 200 nm (insets).

were diluted to 10 μg/ml followed by staining with secondary Alexa-, Cy2-, or Cy3-conjugated goat antimouse antibodies, diluted 1:200.

Immunogold labeling. C6 glioma and MDA-231 breast carcinoma cells, cultured as described above and reaching 80% confluence, were washed (×2) with PBS and fixed (1% glutaraldehyde in 0.1 M cacodylate buffer, pH 7.4) for 10 min at room temperature. Fixative was replaced with fresh glutaraldehyde solution in the same buffer followed by 30 min incubation at RT. Fixed cells were briefly washed and fixed again with 0.5% osmium tetraoxide (OsO_4) for 30 min at RT [34]. Following a brief wash with the same cacodylate buffer, cells were dehydrated with 25, 50, 70, and 90% ethanol for 10 min each, 90 and 95% ethanol for 20 min, and 100% ethanol (×2) for 20 min. Cells were then scraped from the plate, collected into 1.5-ml tubes, equilibrated with propylene oxide, and embedded in embedding resin, as described [34]. Thin sections (60 nm) were then incubated (5 h, RT) with 10 μg/ml of antiheparanase mAb 130 and washed (×5) with Tris-buffered saline (TBS), pH 8.2, containing 20 mM Tris base, 0.9% NaCl, 0.5% BSA, 0.5% Tween 20, and 0.13% NaN_3. Sections were then incubated (30 min, RT) with antimouse IgG-conjugated gold (12 nm) (Sigma, St. Louis, MO), washed (×2) with TBS and (×5) with DDW, and examined with a CM 12 Philips transmission electron microscope (TEM).

Labeling intracellular organelles. Following transfection of human foreskin fibroblasts with pHep2 and pHep-GFP, the cells were incubated with LysoTracker DNA-99 (Molecular Probes, Eugene, OR) at 50 nM in growth medium for 1.5 h at 37°C. Cells were then washed with growth medium and visualized without fixation, as described [35]. Alternatively, cells were fixed and permeabilized with acetone (−20°C, 5 min), followed by immunofluorescent staining of heparanase, as described above.

Digital fluorescence imaging analysis of heparanase subcellular distribution. Images of stained cells were acquired at 3-min intervals for 6 h using an Axioscope microscope (Zeiss, Oberkochen, Germany) equipped with a charge-coupled device (CCD) camera (Model C220, Photometrics Co., Tucson, AZ) with a Texas Instruments 1024 × 1024 pixels chip readout generating 12-bit digital data. The location of individual lysosomes was determined at two time points 9 min apart. This system for computerized microscopy and fluorescence ratio imaging was described in detail elsewhere [36]. In the present study, cells were examined with a 100X/1.3-NA plan Neofluar objective (Zeiss) resulting in a pixel length of 0.118 μm. Corrections for nonhomogenous illumination and pixel-to-pixel variations in CCD sensitivities, as well as aligning the LysoTracker and the GFP images, were routinely performed. The images were

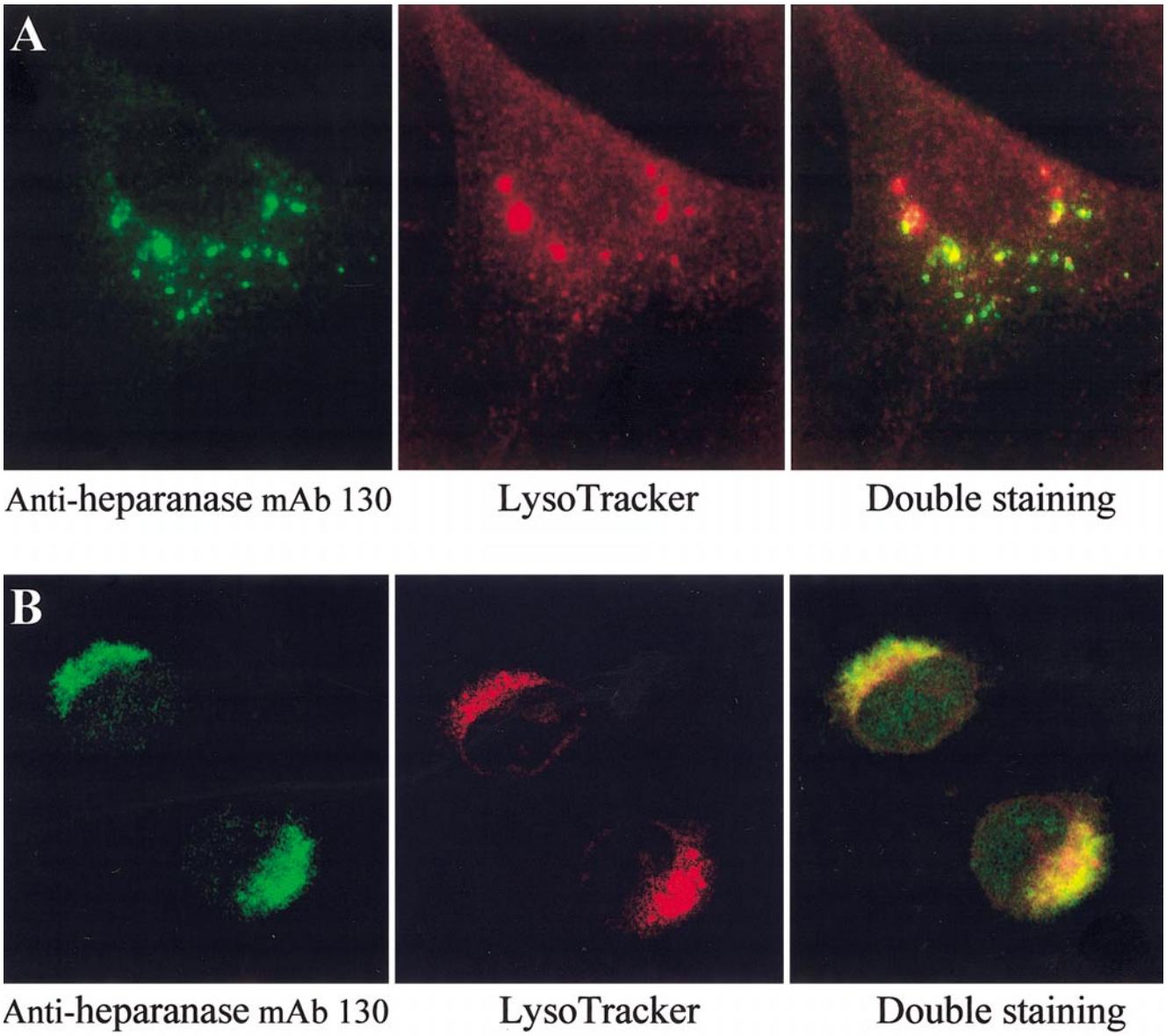

FIG. 3. Heparanase localization in acidic vesicles. (A) Primary human fibroblasts; primary human fibroblasts were transfected with H-*hpa* cDNA and 48 h later subjected to staining of heparanase and lysosomes. (Left) Cells were fixed, permeabilized, and applied to indirect immunofluorescence staining with monoclonal antiheparanase antibodies (mAb 130) followed by Alexa-conjugated goat antimouse antibody (green fluorescence). (Middle) Intact cells were live-stained for 1 h with LysoTracker, labeling acidic organelles, predominantly lysosomes (red fluorescence). (Right) Living cells were first labeled with LysoTracker, followed by fixation, permeabilization, and staining with antiheparanase antibodies. Note the colocalization of heparanase and acidic vesicles (yellow). (B) Localization of endogenous heparanase in MDA-231 cells. (Left) Cells stained with antiheparanase antibodies (mAb 130) followed by Alexa-conjugated goat antimouse antibody (green fluorescence). (Middle) cells live-stained with LysoTracker (red fluorescence). (Right) Cells were labeled with LysoTracker followed by staining with antiheparanase antibodies, as described in A. Note the colocalization of heparanase and acidic vesicles (yellow fluorescence).

then high pass filtered with a box size of 4.7 × 4.7 μm and thresholded to eliminate the background fluorescence.

RESULTS

Expression and Localization of Human Heparanase

In order to evaluate the subcellular localization of heparanase in transfected cells, nonmetastatic C6 rat glioma cells that lack heparanase expression and activity were stable transfected with the full-length human heparanase (H-*hpa*) cDNA. Cell lysates were then assayed for their ability to degrade a biosynthetically labeled ECM (Fig. 1A). Cells transfected with an insert-free pcDNA3 plasmid were used as control. Following incubation on ^{35}S-labeled ECM, the medium was analyzed by gel filtration on Sepharose 6B, as

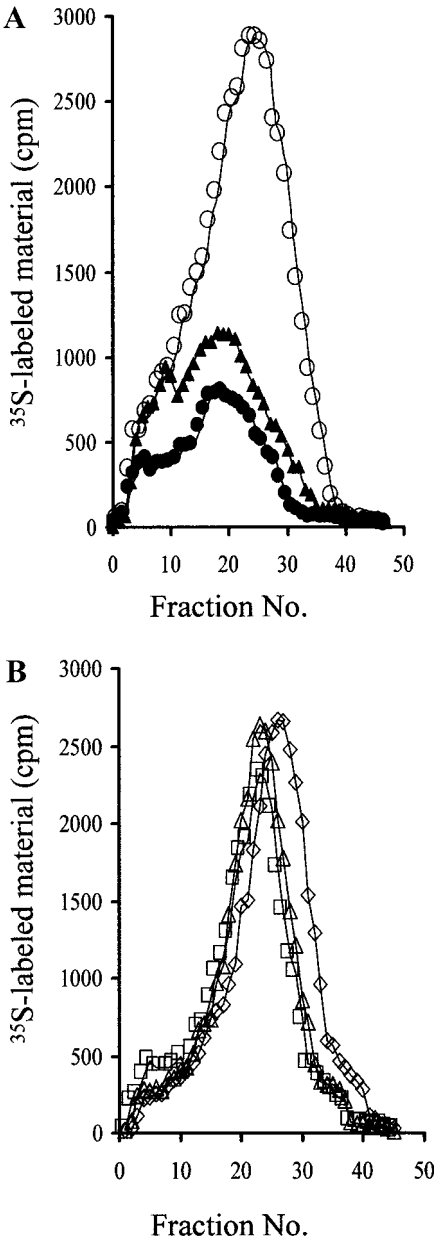

FIG. 4. Heparanase activity depends on the integrity of the Golgi apparatus. (A) Effect of pretreatment with BFA on heparanase activity. Cultured MCF7 cells were incubated (16 h, 37°C) in the absence (○) or the presence of 0.1 (▲) or 10 (●) μg/ml of Brefeldin A. The cells were dissociated with trypsin/EDTA, lysed by three cycles of freezing and thawing, and incubated (24 h, pH 6.0, 2×10^6 cells) with ^{35}S-labeled ECM. Labeled degradation fragments released into the incubation medium were analyzed by gel filtration on Sepharose 6B, as described under Materials and Methods. (B) BFA does not affect recombinant heparanase activity. MCF7 cells were incubated as described above in the absence (◇) or the presence of 1 (□) or 5 (△) μg/ml of BFA. The cells were dissociated and lysed as described in A and then incubated with ^{35}S-labeled ECM in the presence of 10 μg/ml of recombinant heparanase. Labeled degradation fragments released into the incubation medium were analyzed by gel filtration on Sepharose 6B.

described [32]. As demonstrated in Fig. 1A, labeled material released from the ECM by mock-transfected cells eluted just after the void volume (V_0) (peak I, fractions 1–10, $K_{av} < 0.2$) and consisted almost entirely of nearly intact, high-molecular-weight proteoglycans. In contrast, lysates of H-*hpa*-transfected cells degraded the ECM HSPGs as indicated by release of low-molecular-weight labeled degradation fragments that eluted toward the V_t of the column (peak II, fractions 15–30, $0.5 < K_{av} < 0.75$) (Fig. 1A). Labeled fragments eluted in peak II were shown to be degradation products of HS, as they were five- to sixfold smaller than intact HS side chains, resistant to further digestion with papain and chondroitinase ABC, and susceptible to deamination by nitrous acid [32]. Next, we evaluated the subcellular localization of heparanase in the transfected cells by immunofluorescent staining, utilizing antiheparanase mAb 130. In permeabilized cells, heparanase was detected predominantly in a perinuclear, granular pattern (Fig. 1B). In contrast, no staining was detected when fixed unpermeablized cells were incubated with the same antibodies, indicating little or no cell surface localization of the enzyme (not shown). In a subsequent experiment, H-*hpa*-transfected C6 glioma cells and nontransfected MDA-231 breast carcinoma cells expressing endogenous heparanase were subjected to immunogold labeling of heparanase and TEM. Specific heparanase labeling was detected within lysosomes (Figs. 2A–2C, arrows) and the Golgi apparatus (Fig. 2D) of both transfected and nontransfected cells. To further confirm heparanase subcellular localization, we utilized an independent identification method and a different cell type. Primary human foreskin fibroblasts (HFF) that lacked heparanase activity were transfected with H-*hpa*. Forty-eight hours later, the transfected cells were stained by indirect immunofluorescence with antiheparanase antibodies and Alexa-conjugated goat antimouse antibodies. Specific heparanase staining was found exclusively in a granular pattern (Fig. 3A, left). No heparanase staining was detected in nonpermeabilized HFF cells, indicating accumulation of the enzyme in cytoplasmic granules (not shown). In order to determine whether heparanase is indeed localized within lysosomes, intracellular organelles of HFF living cells were first labeled with LysoTracker (a specific fluorescent label of acidic vesicles, predominantly lysosomes) (Fig. 3A, middle). Fixation of these cells followed by indirect immunofluorescent staining with antiheparanase antibodies resulted in colocalization of the LysoTracker with heparanase in the same cytoplasmic granules (Fig. 3A, right), indicating that heparanase is indeed stored within lysosomes. We have also examined heparanase localization in cells that endogenously express the enzyme. For this purpose, nonmetastatic (MCF7) and moderately metastatic (MDA-231) human breast car-

cinoma cells were immunostained with antiheparanase mAb 130. A perinuclear granular staining was observed in both MCF7 (not shown) and MDA-231 (Fig. 3B, left). Staining of living MCF7 and MDA-231 cells with LysoTracker yielded the same cytoplasmic granular staining pattern (Fig. 3B, middle), as also indicated by the colocalization of heparanase and LysoTracker observed in double-stained cells (Fig. 3B, right). Similar results were obtained with the nonmetastatic MCF7 breast carcinoma cells, expressing lower heparanase activity [37]. In both the MCF7 and MDA-231 cells, the cytoplasm is occupied mostly by the nucleus.

Heparanase Activity Depends on the Integrity of the Golgi Apparatus

As demonstrated in Fig. 2, heparanase is localized both in the Golgi apparatus and within lysosomes. In order to examine whether heparanase trafficking via the Golgi is essential for its proper maturation, MCF7 and MDA-231 cells were treated with Brefeldin A (BFA), a drug which dissociates the coat proteins from the trans-Golgi membranes, resulting in disassembly of the Golgi [38]. Briefly, cells were preincubated (16 h, 37°C) with BFA and examined for their heparanase activity. Untreated cells were used as control. As shown in Fig. 4A, heparanase activity was reduced (three- to fourfold) in MCF7 cells treated with 0.1–10 μg/ml of the drug. A similar inhibition was obtained with MDA-231 cells treated with 1–5 μg/ml of BFA (not shown). The three- to fourfold reduction in heparanase activity in BFA-treated cells is in agreement with the relatively short (24–48 h) half life of the heparanase protein, determined in our preliminary pulse–chase experiments performed with 293 cells. It appears that both heparanase and proteases, releasing nearly intact high-molecular-weight HSPGs, are similarly affected by BFA, as indicated by the lack of a significant peak I material in the presence of BFA (Fig. 4A). BFA had a little or no inhibitory effect on heparanase activity when incubated directly with the purified enzyme (not shown) or when BFA-treated cells were lysed and incubated with the recombinant enzyme (Fig. 4B).

Design and Expression of Heparanase-GFP Fusion Protein

In order to study the subcellular localization of heparanase in living cells, we generated heparanase-GFP protein as a complementary research tool to antibody staining (Fig. 5A). Briefly, GFP cDNA was fused to the heparanase C-terminus. Fusion at the C-terminus was imperative since heparanase is synthesized as a latent enzyme of 65 kDa and is proteolytically cleaved at its N-terminus (Gln^{157}–Lys^{158}) to yield a highly active 50-kDa enzyme [26]. Processing at the C-terminus was not identified. It has been postulated that the 50-kDa enzyme forms a heterodimer with an 8-kDa peptide arising from a second proteolytic processing (Gln^{36}–Gln^{109}) of the 65-kDa pre-proheparanase protein [26]. Furthermore, a hydrophobic amino acid stretch at the enzyme N-terminus functions as a signal peptide (Fig. 5A) and the fusion of GFP sequence in this area may interfere with heparanase sub-cellular trafficking. The molecular cloning is described in detail in "Materials and Methods" and resulted in the formation of heparanase-GFP fusion protein driven by a CMV promoter (Fig. 5A).

The heparanase-GFP fusion plasmid was transfected into human foreskin fibroblasts and the cells exhibited heparanase activity when incubated with ^{35}S-labeled ECM (Fig. 5B). Cells transfected with heparanase-GFP were subjected to Western blot analysis to assure that the GFP tag had not been cleaved from the heparanase molecule. A single 84-kDa protein was obtained, representing the 65-kDa heparanase fused to the 20-kDa GFP tag (Fig. 5B, inset). Lower molecular weight bands were not detected by the antiheparanase mAb, indicating that the haparanase-GFP fusion protein was not processed. The observed enzymatic activity may be attributed to a minor fraction of processed heparanase, possibly lacking the GFP tag, but still undetectable by Western blot analysis (measurements of heparanase activity are much more sensitive than Western blotting) or to residual enzymatic activity of the proenzyme. When expressed at low levels, GFP fluorescence was observed in granules spread within the cytoplasm (Fig. 5C, middle), similar to the staining pattern seen with antiheparanase mAb 130. It should be emphasized, however, that neither the heparanase-GFP fusion protein nor the antiheparanase mAb-130 staining could distinguish between the active and latent forms of the enzyme and hence a conclusion regarding the localization of the active enzyme cannot be drawn. In order to characterize the granules containing heparanase-GFP, a LysoTracker marker (a marker for acidic granules, predominantly lysosomes) was added to live HFF transfected with heparanase-GFP. Colocalization of the green fluorescence (GFP) (Fig. 5C, middle) and the red viable staining of the LysoTracker (Fig. 5C, left) was observed, again indicating that heparanase is localized within lysosomal granules (Fig. 5C, right).

The GFP fusion protein was also utilized to study heparanase dynamics within lysosomes of transfected living human primary fibroblasts. For this purpose, the location of individual lysosomes was determined at two time points 9 min apart. As shown in Fig. 6, taken 2 h after the beginning of the recording, lysosomes that contain heparanase were spread throughout the cell, exhibiting a uniform movement toward the direction of the cell leading edge (Fig. 6). No degranulation process

or change in fluorescence intensity of the heparanase-GFP was observed, even following a prolonged (6 h) observation. We therefore suggest that human heparanase storage within lysosomes is apparently stable.

DISCUSSION

Heparan sulfate proteoglycans are major components of the extracellular microenvironment, cell surfaces, and basement membranes. These ubiquitous molecules interact with elements of the basement membrane and provide the ECM with the ability to bind and store growth factors, cytokines, and enzymes [1–4, 39–41]. The extracellular activity of heparanase modulates the molecular structure of the ECM and subendothelial basement membrane, thereby enabling the trans-endothelial migration of normal hematopoietic cells [42] and blood-borne tumor cells [5–10]. In addition, heparanase facilitates the release of heparin-binding growth promoting factors from the ECM [18, 40], thus also acting as a pro-angiogenic factor [9, 18, 43–45]. The extracellular function of heparanase in regulating cellular trafficking and growth factor bioavailability requires its secretion from the cell. However, a heparanase export mechanism(s) should be tightly regulated, since uncontrolled overexpression of the enzyme and the associated inadvertent cleavage of HS may promote tissue damage and pathological processes, such as tumor invasion and metastasis [45], or autoimmune disorders [5, 8–10, 42]. It appears that cellular localization of heparanase plays a role in its activation, regulation, and bioavailability. We have observed that when heparanase is directed to the cell surface, it enhances tumor angiogenesis and the metastatic potential of malignant cells [45]. Similarly, the subcellular localization of cathepsin D and B in breast and bladder cancer cells changes from within lysosomes to the plasma membrane with increasing metastatic potential [46, 47]. Interestingly, we have recently demonstrated that exogenously added recombinant heparanase is readily internalized by human foreskin fibroblasts and accumulates primarily within endosomal structures [48].

Analysis of the human heparanase amino acid sequence indicates the presence of a hydrophobic 35-amino-acid stretch at the N-terminus [6, 11, 27], which may function as a signal peptide, directing the protein to the Golgi apparatus and subsequent secretion. However, our recent immunostaining studies indicated that human heparanase is localized primarily within the cell in a perinuclear granular pattern and is not readily secreted [27]. Replacing the signal peptide of the human heparanase with that of the chicken enzyme resulted in its cell surface localization and efficient secretion [27]. An analysis of the human heparanase signal peptide sequence revealed a significant (~65%, Fig. 7) homology to the signal peptide of the mannose-6-phosphate receptor (M6P-R), responsible for lysosomal trafficking of enzymes [49]. On the other hand, there was a relatively low level of homology (<30%) between the human and chicken heparanase signal peptides (Fig. 7). These data suggest that the signal peptide is essential for subcellular trafficking of heparanase. The homology between the signal sequences of the human enzyme and the M6P-R and the occurrence of a putative small transmembrane sequence at the C-terminus of the human heparanase may imply that the human enzyme could be initially membrane bound. In fact heparanase activity has been previously shown to be partially membrane associated, as revealed by immunostaining [15] and displacement by mannose-6-phosphate [50]. The observed 65% homology between the M6P-R and human heparanase signal sequences may imply that heparanase gets to endosomes by a pathway similar to that of M6P-R and then to the lysosomes by another mechanism. An endogenous, most likely heparanase activity is present in I-cell patient cells [22], implying its lysosomal entry by a M6P-independent pathway.

In the present study, we have identified the localization of heparanase within the lysosomes of three cell types, utilizing three independent methods: immunogold labeling and electron microscopy, colocalization of the enzyme and fluorescent labeled lysosomes, and localization of a fluorescent fusion enzyme within lysosomes of living cells. We have also demonstrated that the integrity of the Golgi apparatus is essential for heparanase activity in MCF7 and MDA-231 breast carcinoma cells, endogenously expressing the enzyme. These results suggest a possible trafficking mechanism in which following synthesis, the enzyme is transported into the Golgi apparatus and subsequently accumulates within lysosomes. Once accumulated, heparanase is apparently stored within these organelles in a stable form, since its activity was readily detected in cell lysates, but was not secreted into the conditioned medium of the transfected cells. In addition, there was no degranulation or trafficking of the enzyme to the cell surface during several hours of observation of living cells expressing fluorescent heparanase (GFP fusion protein) in their lysosomes. Apparently, the acidic microenvironment within lysosomes provides heparanase with suitable conditions for storage and expression of optimal enzymatic activity [19, 20, 51]. Moreover, lysosomes contain a variety of proteolytic enzymes (e.g., cathepsins) that may facilitate the conversion of heparanase from its 65-kDa latent form to the active 50-kDa enzyme and/or the proposed 58-kDa heterodimer heparanase protein [6, 10, 26]. It is therefore suggested that lysosomes may serve as a primary site for heparanase activity and storage. The predominant function attributed to

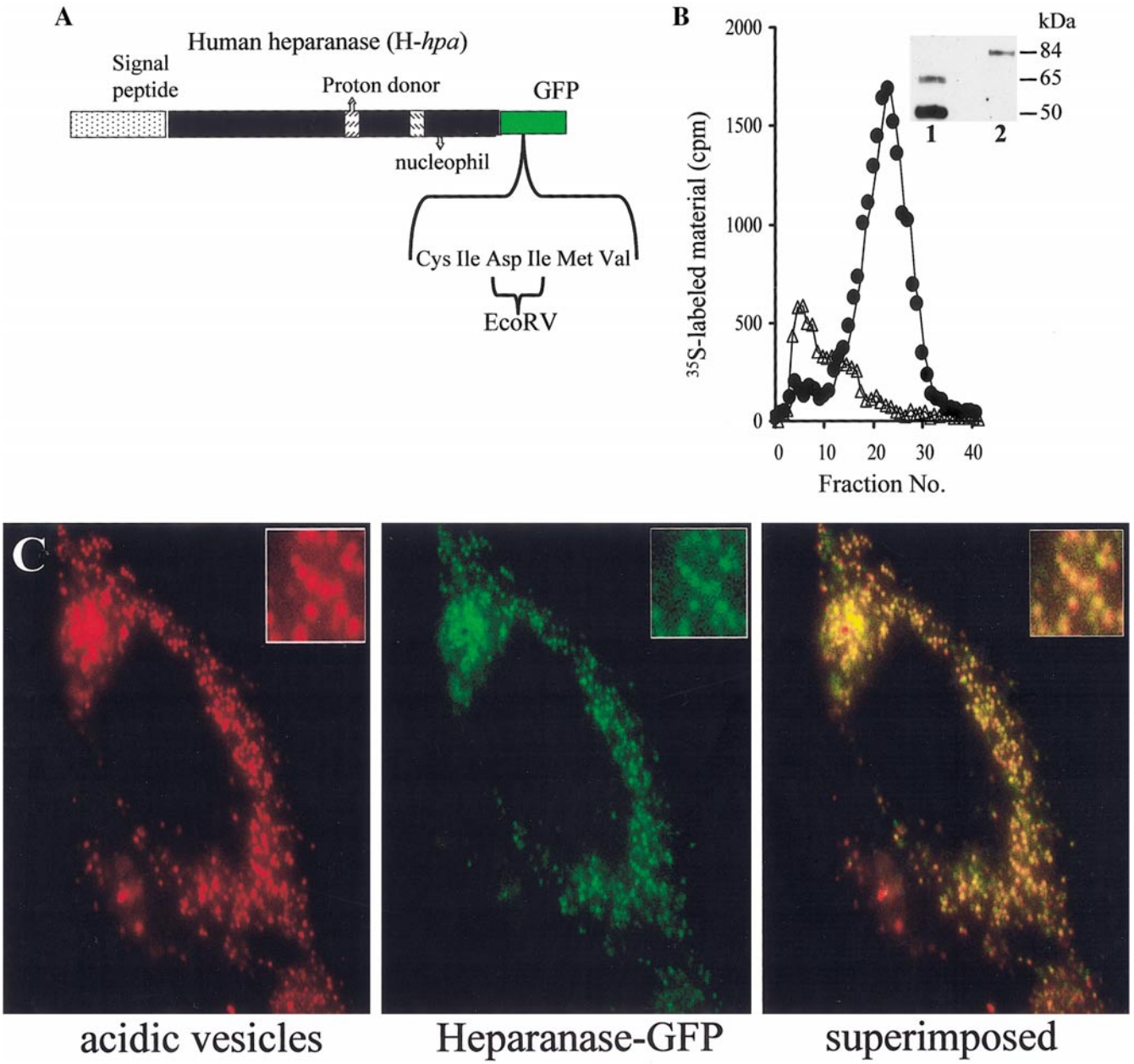

FIG. 5. Generation and expression of heparanase-GFP fusion protein. (A) Heparanase-GFP fusion protein; GFP cDNA was fused to the heparanase C-terminus, as described under Materials and Methods. The resulting expression vector (designated pHep-GFP) contains a CMV promoter, full-length human heparanase cDNA fused in frame with GFP cDNA. Note the position of the signal peptide. (B) Heparanase-GFP activity; primary human fibroblasts transfected with heparanase-GFP (●) or mock transfected (△) were incubated (24 h, pH 6.0, 2×10^6 cells) on ^{35}S-labeled ECM. Labeled degradation fragments released into the incubation medium were analyzed by gel filtration on Sepharose 6B. (Inset) Western blot analysis; primary human fibroblasts were transfected with heparanase-GFP and subjected to immunoblot analysis using antiheparanase mAb-130. Lane 1, recombinant human heparanase showing both the 65- and 50-kDa forms; lane 2, 84-kDa heparananse-GFP fusion protein. (C) Heparanase-GFP expression and localization; primary human fibroblasts were transfected with pHep-GFP. Forty eight hours later, the cells were live-stained for 1 h with LysoTracker. Digital images of GFP-heparanase (middle image, green) or LysoTracker (left image, red) were recorded and superimposed (right image, yellow). Note the colocalization of GFP-heparanase and the acidic vesicles. To exemplify the localization of heparanase in acidic vesicles, an image of several vesicles was magnified and is presented as an inset in each panel.

heparanase is degradation of heparan sulfate proteoglycans in the ECM and basement membranes [7, 9, 10], a function that clearly requires the presence of cell surface-bound and extracellular heparanase. Indeed, heparanase was occasionally detected on the cell surfaces [11, 15] and in several extracellular locations,

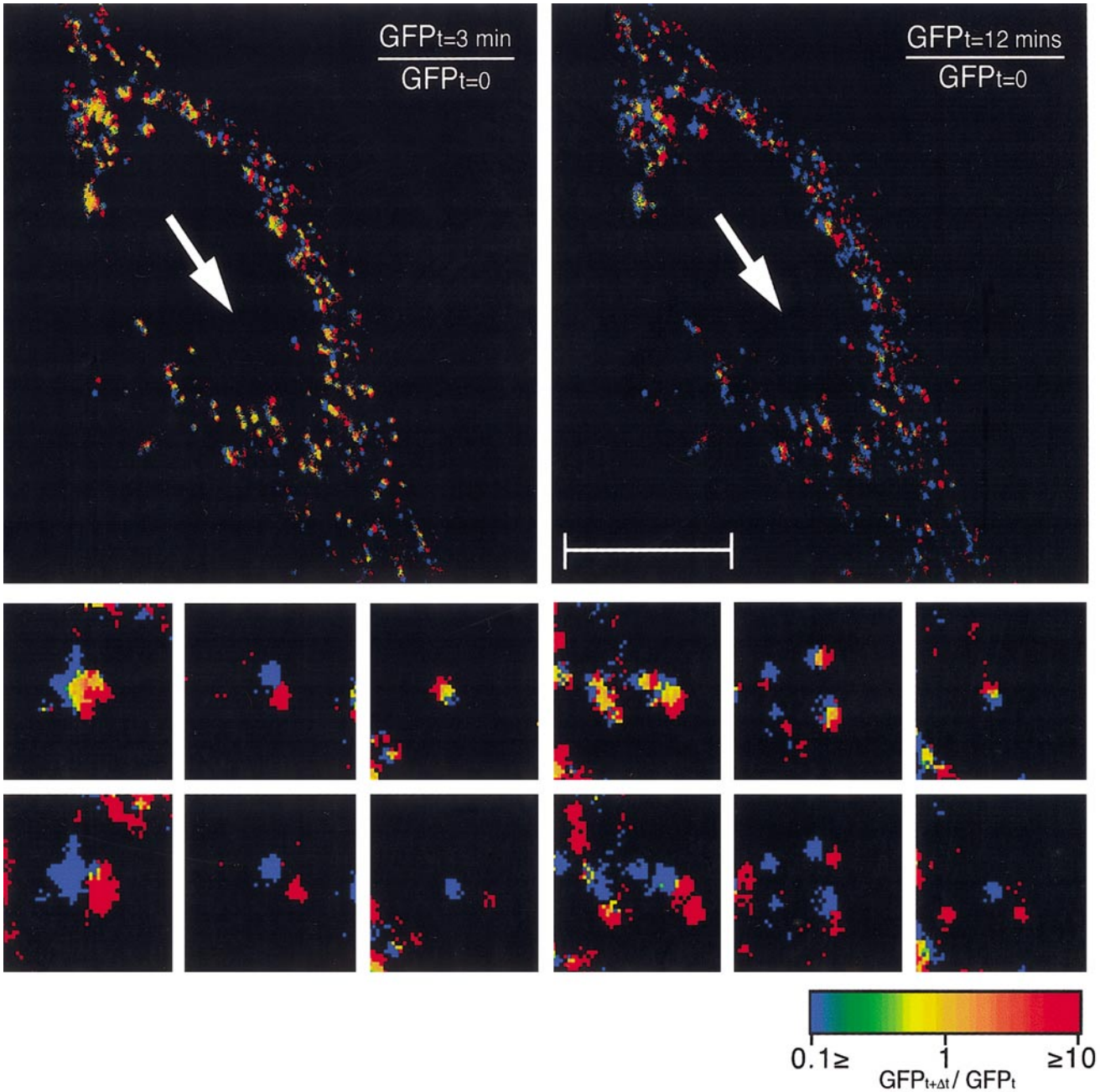

FIG. 6. Temporal changes in localization of heparanase-GFP in transfected human fibroblasts. Living cells were subjected to temporal fluorescence ratio (FRIT) imaging, as described under Materials and Methods. Cells were analyzed by time-lapse recording at 3-min intervals, starting 48 h after transfection with heparanase-GFP. Shown is the fluorescence image obtained 2 h after the beginning of the recording. An identical vesicle array was obtained at 6 h, but the position of the cell was changed, not allowing superimposition of the two images. The dynamic behavior of heparanase-GFP is shown by the FRIT patterns obtained from images taken at 3 (left)- or 12-min (right) intervals. To demonstrate the similar dynamic behavior of heparanase containing vesicles, three representative FRIT images of single vesicles were magnified underneath each complete cell FRIT image. The arrows point toward the leading edge of the cell. Bar, 10 μm.

such as in wound fluid and urine and in close proximity to endothelial cells lining fetal blood vessels [7, 43]. However, we show here that heparanase accumulates predominantly and in a stable manner within the cytoplasm of several cell types. Based on previous studies indicating a strong cytoplasmic staining of heparanase in normal and malignant tissues [15–17, 52], we suggest that apart of its extracellular activities (i.e., cell invasion, release of ECM-bound growth and differentiation factors) heparanase may fulfill intracellular ac-

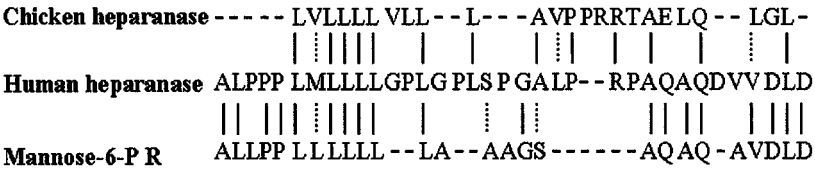

FIG. 7. Signal peptide sequence alignment. Heparanase 5′ cDNA encodes for a 35-amino-acid putative signal peptide. There is a relatively high homology (~65%) between the human heparanase signal peptide and the signal peptide of the mannose-6-phosphate receptor (mannose-6-PR), responsible for lysosomal trafficking of enzymes, vs a relatively low level of homology (<30%) with the chicken heparanase signal peptide.

tivities, such as regulation of HSPG turnover and metabolism, known to be associated with lysosomal functions [20, 21]. Also, as indicated in previous studies, acidic pH is essential for optimal heparanase activity [51, 53]. It has been previously proposed that HS is degraded stepwise in endosomal (chloroquine insensitive) and then further in lysosomal compartments [54, 55]. A more recent study, demonstrated, however, that HS degradation occurs only in lysosomes and late endosomes [56], supporting our observations. It should be pointed out, however, that both the LysoTracker dye and electron microscopy analysis used in this study fail to distinguish between late endosomes and lysosomes. Hence, the actual sequence and sites of HS degradation cannot be determined based on the present study. Taken together, it is conceivable that the lysosomal compartment may serve as the predominant subcellular site for heparanase confinement within the cell, preventing its uncontrolled extracellular activity associated, for example, with cancer progression and autoimmune disorders.

We thank Dr. I. Pecker, Dr. Orom Yacoby-Zeevi (InSight Ltd., Rehovot, Isarel), Dr. M. Trashis, and Dr. E. Rachamim (Hadassah-University Medical School) for their helpful suggestions and excellent assistance and Insight Ltd. for providing the antihuman heparanase antibodies (mAb 130). This work was supported by the Israel Science Foundation (Grant 503/98); the Association for International Cancer Research, UK; the NIH (R21 CA87085); and the U.S. Army (Grant 0278).

REFERENCES

1. Bernfield, M., Gotte, M., Park, P. W., Reizes, O., Fitzgerald, M. L., Lincecum, J., and Zako, M. (1999). Functions of cell surface heparan sulfate proteoglycans. *Annu. Rev. Biochem.* **68,** 729–777.
2. Vlodavsky, I., Bar-Shavit, R., Korner, G., and Fuks, Z. (1993). Extracellular matrix-bound growth factors, enzymes and plasma proteins. *In* "Molecular and Cellular Aspects of Basement Membranes" (D. H. Rohrbach and R. Timpl, Eds.), pp. 327–343, Academic Press, Orlando, Fl.
3. Kjellen, L., and Lindahl, U. (1991). Proteoglycans: Structures and interactions. *Annu. Rev. Biochem.* **60,** 443–475.
4. Iozzo, R. V. (1998). Matrix proteoglycans: from molecular design to cellular function. *Annu. Rev. Biochem.* **67,** 609–652.
5. Vlodavsky, I., Mohsen, M., Lider, O., Svahn, C. M., Ekre, H. P., Vigoda, M., Ishai-Michaeli, R., and Peretz, T. (1994). Inhibition of tumor metastasis by heparanase inhibiting species of heparin. *Invasion Metastasis* **14,** 290–302.
6. Vlodavsky, I., Friedmann, Y., Elkin, M., Aingorn, H., Atzmon, R., Ishai-Michaeli, R., Bitan, M., Pappo, O., Peretz, T., Michal, I., Spector, L., and Pecker, I. (1999). Mammalian heparanase: Gene cloning, expression and function in tumor progression and metastasis. *Nature Med.* **5,** 793–802.
7. Dempsey, L. A., Plummer, T. B., Coombes, S. L., and Platt, J. L. (2000). Heparanase expression in invasive trophoblasts and acute vascular damage. *Glycobiology* **10,** 467–475.
8. Nakajima, M., Irimura, T., and Nicolson, G. L. (1988). Heparanases and tumor metastasis. *J. Cell Biochem.* **36,** 157–167.
9. Vlodavsky, I., and Friedmann, Y. (2001). Molecular properties and involvement of heparanase in cancer metastasis and angiogenesis. *J. Clin. Invest.* **108,** 341–347.
10. Parish, C. R., Freeman, C., and Hulett, M. D. (2001). Heparanase: A key enzyme involved in cell invasion. *Biochim. Biophys. Acta* **1471,** M99–108.
11. Hulett, M. D., Freeman, C., Hamdorf, B. J., Baker, R. T., Harris, M. J., and Parish, C. R. (1999). Cloning of mammalian heparanase, an important enzyme in tumor invasion and metastasis. *Nat. Med.* **5,** 803–809.
12. Kussie, P. H., Hulmes, J. D., Ludwig, D. L., Patel, S., Navarro, E. C., Seddon, A. P., Giorgio, N. A., and Bohlen, P. (1999). Cloning and functional expression of a human heparanase gene. *Biochem. Biophys. Res. Commun.* **261,** 183–187.
13. Toyoshima, M., and Nakajima, M. (1999). Human heparanase. Purification, characterization, cloning, and expression. *J. Biol. Chem.* **274,** 24153–24160.
14. Pikas, D. S., Li, J. P., Vlodavsky, I., and Lindahl, U. (1998). Substrate specificity of heparanases from human hepatoma and platelets. *J. Biol. Chem.* **273,** 18770–18777.
15. Friedmann, Y., Vlodavsky, I., Aingorn, H., Aviv, A., Peretz, T., Pecker, I., and Pappo, O. (2000). Expression of heparanase in normal, dysplastic, and neoplastic human colonic mucosa and stroma. Evidence for its role in colonic tumorigenesis. *Am. J. Pathol.* **157,** 1167–1175.
16. Gohji, K., Okamoto, M., Kitazawa, S., Toyoshima, M., Dong, J., Katsuoka, Y., and Nakajima, M. (2001). Heparanase protein and gene expression in bladder cancer. *J. Urol.* **166,** 1286–1290.
17. Koliopanos, A., Friess, H., Kleeff, J., Shi, X., Liao, Q., Pecker, I., Vlodavsky, I., Zimmermann, A., and Buchler, M. W. (2001). Heparanase expression in primary and metastatic pancreatic cancer. *Cancer Res.* **61,** 4655–4659.
18. Elkin, M., Ilan, N., Ishai-Michaeli, R., Friedmann, Y., Papo, O., Pecker, I., and Vlodavsky, I. (2001). Heparanase as mediator of angiogenesis: Mode of action. *FASEB J.* **15,** 1661–1663.

19. Hook, M., Wasteson, A., and Oldberg, A. (1975). A heparan sulfate-degrading endoglycosidase from rat liver tissue. *Biochem. Biophys. Res. Commun.* **67,** 1422–1428.
20. Kjellen, L., Pertoft, H., Oldberg, A., and Hook, M. (1985). Oligosaccharides generated by an endoglucuronidase are intermediates in the intracellular degradation of heparan sulfate proteoglycans. *J. Biol. Chem.* **260,** 8416–8422.
21. Yanagishita, M., and Hascall, V. C. (1992). Cell surface heparan sulfate proteoglycans. *J. Biol. Chem.* **267,** 9451–9454.
22. Brauker, J. H., and Wang, J. L. (1987). Nonlysosomal processing of cell-surface heparan sulfate proteoglycans. Studies of I-cells and NH_4Cl-treated normal cells. *J. Biol. Chem.* **262,** 13093–13101.
23. Bame, K. J. (2001). Heparanases: Endoglycosidases that degrade heparan sulfate proteoglycans. *Glycobiology* **11,** 91R–98R.
24. Mollinedo, F., Nakajima, M., Llorens, A., Barbosa, E., Callejo, S., Gajate, C., and Fabra, A. (1997). Major co-localization of the extracellular-matrix degradative enzymes heparanase and gelatinase in tertiary granules of human neutrophils. *Biochem. J.* **327,** 917–923.
25. Matzner, Y., Vlodavsky, I., Bar-Ner, M., Ishai-Michaeli, R., and Tauber, A. I. (1992). Subcellular localization of heparanase in human neutrophils. *J. Leukocyte Biol.* **51,** 519–524.
26. Fairbanks, M. B., Mildner, A. M., Leone, J. W., Cavey, G. S., Mathews, W. R., Drong, R. F., Slightom, J. L., Bienkowski, M. J., Smith, C. W., Bannow, C. A., and Heinrikson, R. L. (1999). Processing of the human heparanase precursor and evidence that the active enzyme is a heterodimer. *J. Biol. Chem.* **274,** 29587–29590.
27. Goldshmidt, O., Zcharia, E., Aingorn, H., Guatta-Rangini, Z., Atzmon, R., Michal, I., Pecker, I., Mitrani, E., and Vlodavsky, I. (2001). Expression pattern and secretion of human and chicken heparanase are determined by their signal peptide sequence. *J. Biol. Chem.* **276,** 29178–29187.
28. Sambrook, J., Fritsch, E. F., and Maniatis, T. (1989). "Molecular Cloning, A Laboratory Manual," Cold Spring Harbor Laboratory Press, Cold Spring Harbor, NY.
29. Katz, B. Z., Krylov, D., Aota, S., Olive, M., Vinson, C., and Yamada, K. M. (1998). Green fluorescent protein labeling of cytoskeletal structures—Novel targeting approach based on leucine zippers. *Biotechniques* **25,** 298–302.
30. LaFlamme, S. E., Thomas, L. A., Yamada, S. S., and Yamada, K. M. (1994). Single subunit chimeric integrins as mimics and inhibitors of endogenous integrin functions in receptor localization, cell spreading and migration, and matrix assembly. *J. Cell Biol.* **126,** 1287–1298.
31. Vlodavsky, I. (1999). Preparation of extracellular matrices produced by cultured corneal endothelial and PF-HR9 endodermal cells. *In* "Current Protocols in Cell Biology," Vol. 1, pp. 10.4.1–10.4.14, Wiley, New York.
32. Vlodavsky, I., Fuks, Z., Bar-Ner, M., Ariav, Y., and Schirrmacher, V. (1983). Lymphoma cell-mediated degradation of sulfated proteoglycans in the subendothelial extracellular matrix: Relationship to tumor cell metastasis. *Cancer Res.* **43,** 2704–2711.
33. Katz, B. Z., Levenberg, S., Yamada, K. M., and Geiger, B. (1998). Modulation of cell-cell adherens junctions by surface clustering of the N-cadherin cytoplasmic tail. *Exp. Cell Res.* **243,** 415–424.
34. Castel, M., Belenky, M., Cohen, S., Ottersen, O. P., and Storm-Mathisen, J. (1993). Glutamate-like immunoreactivity in retinal terminals of the mouse suprachiasmatic nucleus. *Eur. J. Neurosci.* **5,** 368–381.
35. Zamir, E., Katz, M., Posen, Y., Erez, N., Yamada, K. M., Katz, B. Z., Lin, S., Lin, D. C., Bershadsky, A., Kam, Z., and Geiger, B. (2000). Dynamics and segregation of cell-matrix adhesions in cultured fibroblasts. *Nat. Cell Biol.* **2,** 191–196.
36. Zamir, E., Katz, B. Z., Aota, S., Yamada, K. M., Geiger, B., and Kam, Z. (1999). Molecular diversity of cell-matrix adhesions. *J. Cell Sci.* **112,** 1655–1669.
37. Zcharia, E., Metzger, S., Chajek-Shaul, T., Friedmann, Y., Pappo, O., Aviv, A., Elkin, M., Pecker, I., Peretz, T., and Vlodavsky, I. (2001). Molecular properties and involvement of heparanase in cancer progression and mammary gland morphogenesis. *J. Mamm. Gland Biol. Neoplasia* **6,** 311–322.
38. Ward, T. H., Polishchuk, R. S., Caplan, S., Hirschberg, K., and Lippincott-Schwartz, J. (2001). Maintenance of Golgi structure and function depends on the integrity of ER export. *J. Cell Biol.* **155,** 557–570.
39. Wight, T. N., Kinsella, M. G., and Qwarnstrom, E. E. (1992). The role of proteoglycans in cell adhesion, migration and proliferation. *Curr. Opin. Cell Biol.* **4,** 793–801.
40. Vlodavsky, I., Bar-Shavit, R., Ishai-Michaeli, R., Bashkin, P., and Fuks, Z. (1991). Extracellular sequestration and release of fibroblast growth factor: A regulatory mechanism? *Trends Biochem. Sci.* **16,** 268–271.
41. Gupta, P., Oegema, T. R., Jr., Brazil, J. J., Dudek, A. Z., Slungaard, A., and Verfaillie, C. M. (1998). Structurally specific heparan sulfates support primitive human hematopoiesis by formation of a multimolecular stem cell niche. *Blood* **92,** 4641–4651.
42. Vlodavsky, I., Eldor, A., Haimovitz-Friedman, A., Matzner, Y., Ishai-Michaeli, R., Lider, O., Naparstek, Y., Cohen, I. R., and Fuks, Z. (1992). Expression of heparanase by platelets and circulating cells of the immune system: Possible involvement in diapedesis and extravasation. *Invasion Metastasis* **12,** 112–127.
43. Vlodavsky, I., Miao, H.-Q., Benezra, M., Lider, O., Bar-Shavit, R., Schmidt, A., and Peretz, T. (1997). Involvement of the extracellular matrix, heparan sulfate proteoglycans and heparan sulfate degrading enzymes in angiogenesis and metastasis. *In* "Tumor Angiogenesis" (C. E. Lewis, R. Bicknell, and N. Ferrara, Eds.), pp. 125–140, Oxford Univ. Press, Oxford UK.
44. Vlodavsky, I., Miao, H. Q., Medalion, B., Danagher, P., and Ron, D. (1996). Involvement of heparan sulfate and related molecules in sequestration and growth promoting activity of fibroblast growth factor. *Cancer Metastasis Rev.* **15,** 177–186.
45. Goldhsmidt, O., Zcharia, E., Abramovitch, A., Metzger, S., Aingorn, H., Friedmann, Y., Schirrmacher, V., Mitrani, E., and Vlodavsky, I. (2002). Cell surface expression and secretion of heparanase markedly promote tumor angiogenesis and metastasis. *Proc. Nat. Acad. Sci. USA* **99,** 10031–10036.
46. Rochefort, H., Liaudet, E., and Garcia, M. (1996). Alterations and role of human cathepsin D in cancer metastasis. *Enzyme Protein* **49,** 106–116.
47. Sloane, B. F., Moin, K., Sameni, M., Tait, L. R., Rozhin, J., and Ziegler, G. (1994). Membrane association of cathepsin B can be induced by transfection of human breast epithelial cells with c-Ha-ras oncogene. *J. Cell Sci.* **107,** 373–384.
48. Nadav. L., Eldor, A., Yacoby-Zeevi, O., Zamir, E., Pecker, I., Ilan, N., Vlodavsky, I., and Katz, B. (2002). Activation, processing and trafficking of extracellular heparanase by primary human fibroblasts. *J. Cell Sci.* **115,** 2179–2187.
49. Wendland, M., von Figura, K., and Pohlmann, R. (1991). Mutational analysis of disulfide bridges in the Mr 46,000 mannose 6-phosphate receptor. Localization and role for ligand binding. *J. Biol. Chem.* **266,** 7132–7136.
50. Bartlett, M. R., Cowden, W. B., and Parish, C. R. (1995). Differential effects of the anti-inflammatory compounds heparin,

mannose-6-phosphate, and castanospermine on degradation of the vascular basement membrane by leukocytes, endothelial cells, and platelets. *J. Leukocyte Biol.* **57,** 207–213.

51. Gilat, D., Hershkoviz, R., Goldkorn, I., Cahalon, L., Korner, G., Vlodavsky, I., and Lider, O. (1995). Molecular behavior adapts to context: heparanase functions as an extracellular matrix-degrading enzyme or as a T cell adhesion molecule, depending on the local pH. *J. Exp. Med.* **181,** 1929–1934.
52. Bernard, D., Mehul, B., Delattre, C., Simonetti, L., Thomas-Collignon, A., and Schmidt, R. (2001). Purification and characterization of the endoglycosidase heparanase 1 from human plantar stratum corneum: a key enzyme in epidermal physiology? *J. Invest. Dermatol.* **117,** 1266–1273.
53. Nakajima, M., Irimura, T., Di Ferrante, D., Di Ferrante, N., and Nicolson, G. L. (1983). Heparan sulfate degradation: Relation to tumor invasive and metastatic properties of mouse B16 melanoma sublines. *Science* **220,** 611–613.
54. Iozzo, R. (1987). Turnover of heparan sulfate proteoglycan in human colon carcinoma cells. A quantitative biochemical and autoradiographic study. *J. Biol. Chem.* **262,** 1888–1900.
55. Yanagishita, M. (1985). Inhibition of intracellular degradation of proteoglycans by leupeptin in rat ovarian granulose cells. *J. Biol. Chem.* **260,** 11075–11082.
56. Egeberg, M. (2001). Internalization and stepwise degradation of heparan sulfate proteoglycans in rat hepatocytes. *Biochim. Biophys. Acta* **1541,** 135–149.

Received March 11, 2002
Revised version received August 19, 2002
Published online October 11, 2002